STScI | SPACE TELESCOPE SCIENCE INSTITUTE

Instrument Science Report ACS 2020-05

Anneal Efficacy in the Advanced Camera for Surveys Wide Field Channel

M. C. McDonald, T. D. Desjardins, N. D. Miles

April 30, 2020

Abstract

The population of hot pixels in the Advanced Camera for Surveys (ACS) Wide Field Channel (WFC) has been shown to be temporarily reduced by a monthly annealing process. In this report, we investigate the incidence and frequency of hot pixels, from the installation of ACS on the Hubble Space Telescope in 2002 to mid 2019, to assess the efficacy of anneals in reducing the overall dark current and total number of hot pixels in the WFC CCD detectors. An inspection of calibrated and combined raw dark frames taken directly before and after each anneal imply less effective hot pixel healing in recent years, with several post-anneal darks having a higher dark current rate and hot pixel count than their pre-anneal counterparts. The percent hot pixel coverage is tracked using individual calibrated dark frames over a four-year period from 2015 to 2019. We find a characteristic zig-zag shape, indicative of the periodic rise and fall of hot pixel coverage over several anneal cycles, but with lots of scatter between anneal dates. Finally, the dark current of a single, stable, frequently hot pixel is mapped to reveal significant variations, up to 2.0 e^-/s, over the span of several years.

1 Introduction

The Advanced Camera for Surveys (ACS) Wide Field Channel (WFC) is continuously exposed to damaging radiation in the Low Earth Orbit of the Hubble Space Telescope. As

energetic particles from space interact with silicon atoms in the CCD lattice, the detector suffers from displacement damage and excess thermal charge is trapped. This excess charge, known as dark current (e.g., Borncamp et al. 2017), is measured through the inspection of dark frames, i.e., images taken with the camera shutter closed so that the primary signal generated is that of the thermal activity of the detector itself. Once the dark current of a single pixel reaches 0.14 e^-/s, that pixel is then considered to be hot and its dark current can be either stable or unstable over time. A hot pixel with a dark current that changes very little between exposures over an anneal period (i.e., the time in-between anneals) is classified as stable, whereas a hot pixel with a dark current that fluctuates by more than the allowed value (see Borncamp et al. 2017) over an anneal period is classified as unstable. Stable hot pixels are calibratable, though noisier than their cold counterparts.

The dark current and number of stable hot pixels in the ACS/WFC is expected to increase linearly over time (Golimowski et al., 2011). The population of hot pixels is temporarily reduced after a 12-hour annealing process, taking place approximately every 4 weeks, where the detector's thermo-electric coolers are turned off and the CCD is heated from its operating temperature of -81°C to +20°C. The specific mechanism during the annealing process that reduces dark current in pixels is not well understood. This process repairs only a portion of the damaged silicon lattice (Desjardins et al., 2018) and there remains a subset of permanently hot pixels that currently make up about 2% of the detector. The accumulation and intensity of these hot pixels are the focus of this report, in which we intend to investigate the efficacy of ACS anneals at various points in its history and examine how annealing efficacy scales with the level of displacement damage.

1.1 Brief History of the ACS Anneal

While the annealing process, with some variations, has taken place since the installation of ACS in 2002, not all anneals have been carried out under the same conditions. The duration of the anneal has been adjusted over the lifetime of ACS, ranging anywhere from 6 hours to 24 hours (Desjardins et al., 2018). In February 2005, the anneal duration was switched from 12 hours to 6 hours and anneals continued this way until the Side-2 electronics failure in January 2007. The 12-hour anneals were resumed after the recovery of ACS/WFC via Servicing Mission 4 (SM4) in May 2009, after data indicated that the reduced anneal duration resulted in faster growing dark current during that time period. In addition, the malfunction of Side-1 electronics in June 2006 prompted the switch to Side-2 electronics when operations were recovered; a change that gave the ACS team the opportunity to lower the CCD operating temperature from -77°C to -81°C (Sirianni et al., 2006). This reduction in temperature significantly reduced the dark current rate and -81°C has remained the intended operating temperature ever since.

2 Data and Analysis

In this section we describe the two approaches used to assess anneal efficacy: a long-term pre- and post-anneal analysis and an examination of individual dark frames over the four-year time span from January 2015 to January 2019.

2.1 Pre- and Post-Anneal

As requested in the CCD Hot Pixel Annealing program, a set of darks and biases are taken before and after each anneal to monitor the efficacy of that anneal. With the exception of the first few programs (HST proposals 9031, 9566, 9650, and 10046; PI: Cox), four 1000- or 1040-second dark frames were collected pre- and post-anneal over the lifetime of ACS. The window of time to collect these frames has also changed throughout the years: frames were taken within 72 hours before and after each anneal from March 2002 to September 2004, within 12 hours before and after each anneal from October 2004 to August 2009, and within 12 hours before and 6-18 hours after each anneal from August 2009 to present. Despite the differences in exposure and scheduling, this large sample of dark frames provides a consistent record of pre- and post-anneal data that allows for a thorough comparative analysis.

After collecting 1,355 raw darks taken as part of the CCD Hot Pixel Annealing programs from March 2002 to August 2019, we used the CALACS code `acsccd` to subtract the bias level from each frame, producing intermediate blv_tmp.fits files. Then, we sorted the bias-subtracted files into 'before' and 'after' groups according to their corresponding anneal date. Each group was then combined and cosmic ray rejected using the CALACS code `acsrej`, leaving one pre-anneal stack and one post-anneal stack for almost every anneal during this time frame. For various reasons, certain pre- or post-anneal darks were lost or omitted entirely. For example, the pre-anneal darks were omitted from December 2002 to October 2004 for no specific reason at all, as detailed in proposals 9650 (Cox, 2002) and 10046 (Cox, 2003).

The final data sample consisted of 168 pre-anneal and 190 post-anneal stacks. From these data, we measure the mean and median dark current pre- and post-anneal of the whole WFC detector, as well as with respect to each of the readout amplifiers A, B, C and D. In addition, we measure the total number of hot pixels pre- and post-anneal, and the change in hot pixels (*post-anneal* − *pre-anneal*) for each anneal period.

2.2 Individual Dark Frames

On Monday, Wednesday and Friday of each week since January 15, 2015, four 1000.5 second (long) exposure dark frames and two 0.5079 second (short) exposure dark frames are taken as part of the CCD Daily Monitor program. These frequent snapshots of the WFC dark rate enabled us to track the behavior of hot pixels in between anneal periods on a frame-by-frame basis. In this study, we focused on the long daily monitor darks from January 2015 to January 2019, which comprised 2,363 frames in total.

The raw dark files were run through CALACS, producing bias- and flash-subtracted flt.fits files. The total number of hot pixels in each file were identified by first rejecting any cosmic rays present based on if a single pixel exceeded the defined threshold of 0.14 e^-/s and if the signal spread to three or more surrounding pixels. Any pixel detected above this threshold that did not also meet the cosmic ray spatial criteria was deemed a hot pixel. Along with the total number of hot pixels in each frame, the x and y position and signal (in electrons) of each individual hot pixel were also measured.

Among the 2,363 long dark images spanning over the four-year period, over 568 million hot pixels, and their respective coordinates and signal, were identified. This immense data

set required more efficient and organized handling, for which we employed a MySQL database (`acs_monitor_db`). We set up two tables in this database, the first named `hps_image` which contained the filename, modified julian date (mjd) and exposure time for each file in the data set. The second table created, `hps_pixels`, contained the signal, x position, y position and corresponding filename for each hot pixel identified. A single, stable, frequently hot pixel was identified at $(x, y) = (1583, 3950)$ and its dark current was measured.

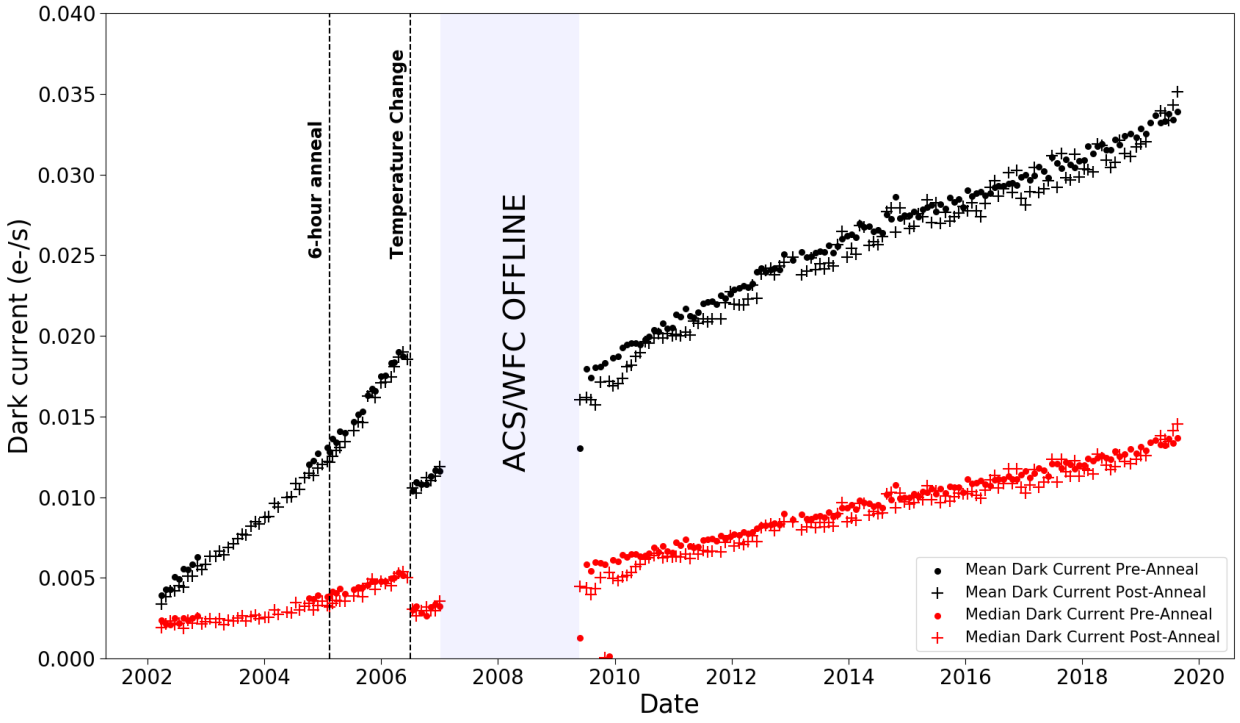

Figure 1: Pre- and post-anneal mean and median dark currents are plotted in black and red, respectively. Filled circles indicate pre-anneal values and crosses indicate post-anneal values. Each data point is a calibrated and combined set of darks from the CCD Hot Pixel Annealing Program. The dashed vertical lines indicate the test of the 6-hour anneals and the reduction in operating temperature as a result of the Side-1 electronics failure (Section 1.1). The blue rectangle denotes the time period in which Side-2 electronics failed and ACS was offline until recovery via SM4 in May 2009 (Section 1.1).

3 Results

The pre- and post-anneal mean and median dark currents for the ACS/WFC are plotted in Figure 1. Immediately, we observe several noticeable features in the dark current measurements. First, both the mean and median dark current rates increase in a similar manner, with the mean increasing from about 0.003 to 0.035 e^-/s and the median increasing from about 0.002 to 0.014 e^-/s. Second, we re-confirm that certain changes to anneal conditions drastically affect the dark rate: 1) The switch to 6-hour anneals in February 2005 increased the slope of the dark current for the duration in which they were carried out (see Table 1) and 2) the reduction in operating temperature in June 2006 from -77 to -81°C significantly lowered the dark current. Finally, we identify several instances in the last several years

where post-anneal dark current rates are greater than their corresponding pre-anneal rates; an effect we do not fully understand the cause of.

Table 1: Dark Current Slope Comparison

Dates	Mean (e^-/s)		Median (e^-/s)	
	Pre-Anneal	Post-Anneal	Pre-Anneal	Post-Anneal
Launch - Jan 2005	8.670e-06	8.328e-06	1.670e-06	1.301e-06
Feb 2005[a]- June 2006[b]	1.344e-05	1.478e-05	2.724e-06	4.338e-06
July 2006 - Jan 2007[c]	6.883e-06	7.948e-06	1.719e-06	2.629e-06
May 2009[d]- Aug 2019	4.386e-06	4.564e-06	2.200e-06	2.321e-06

[a] Anneal duration was switched from 12 hours to 6 hours.
[b] The last anneal before the Side-1 electronics failure, which also coincided with the reduction in operating temperature from -77 to -81°C.
[c] The last anneal before the Side-2 electronics failure, resulting in the loss of ACS/WFC functionality.
[d] The ACS/WFC was recovered via SM4 and 12-hour anneals were resumed.

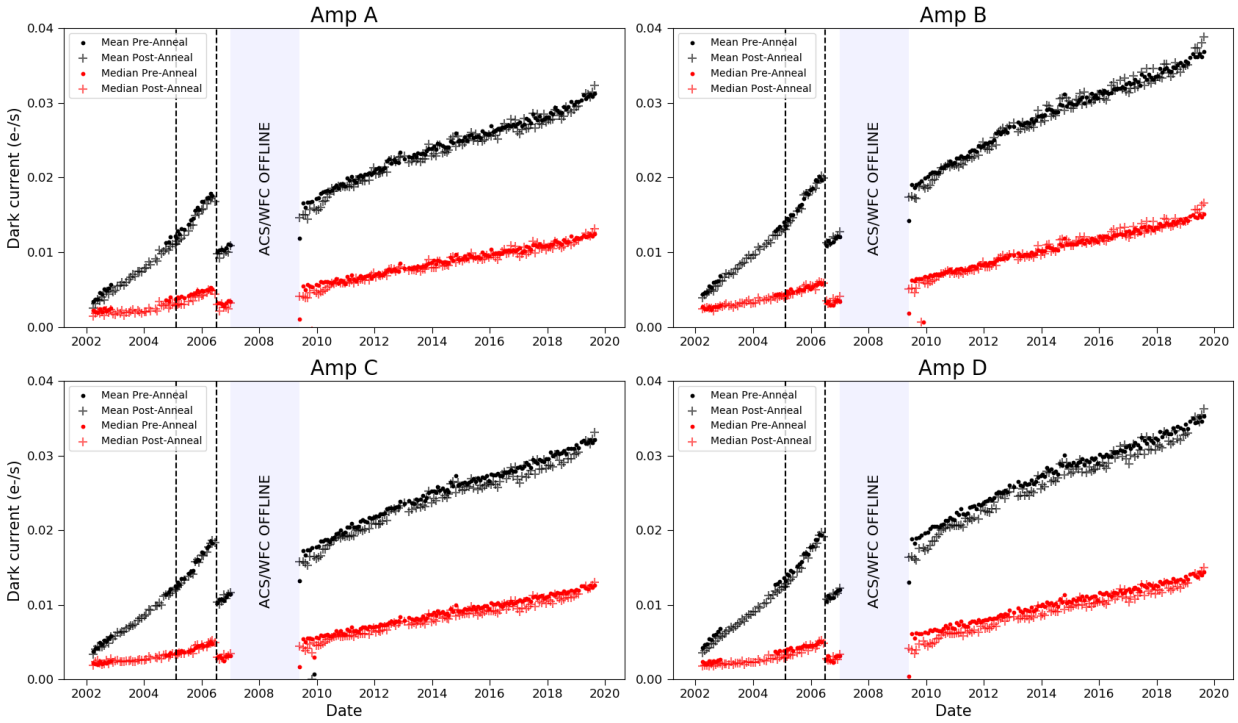

Figure 2: Mean and median dark currents measured with respect to readout amplifiers A, B, C and D. Similar to Figure 1, data points in black represent the mean and red the median, while filled circles and crosses indicate pre- and post-anneal values, respectively. All graph features including dashed lines and rectangles retain the same meaning as in explained in Figure 1.

To better understand how dark current is distributed on the CCD, the mean and median dark currents are measured with respect to readout amplifiers A, B, C, and D. The results, plotted in Figure 2, display many of the same features as those seen in Figure 1. Refer to

Table 2: Max Dark Current by Readout Amplifier

Readout Amplifier	Mean (e^-/s)	Median (e^-/s)
A	0.03232	0.01312
B	0.03884	0.01662
C	0.03309	0.01301
D	0.03629	0.01503

Table 2 for measurements of the maximum mean and median dark current with respect to each readout amplifier. We observe the dark current rates in readout amplifier B to be the greatest, followed by readout amplifiers D, C and A.

The total number of hot pixels pre- and post-anneal are plotted in Figure 3 along with the corresponding change in hot pixels for each anneal period. Like the mean and median dark current rates, we observe steadily increasing behavior in the total number of hot pixels, with the count close to zero shortly after launch and increasing to almost 250,000 hot pixels in August 2019. Along with displaying many of the same features as Figures 1 and 2, Figure 3 more clearly illustrates how many recent post-anneal measurements are greater than their pre-anneal counterparts. In particular, starting around the year 2013, the change in hot pixels more frequently rises above zero, indicating a greater number of hot pixels after those anneals, than beforehand.

On an individual dark frame basis, Figure 5 shows the percent hot pixel coverage of the ACS/WFC CCDs from January 2015-2019. The vertical, blue lines indicate the occurrence of an anneal. Each point on the plot is derived from the total hot pixel count from a single, Daily Monitor long dark frame. Figure 5 shows a steady climb in percent hot pixel coverage over the four-year period, increasing from just above 1.2% in 2015 to just under 1.5% in 2019. The high variability between anneal periods is also illustrated nicely in this plot, with the range in percent hot pixel coverage exceeding 0.1% for several anneal periods. Overall, we do see a zig-zag trend in the data, similar, but not identical to, the ACS/WFC sawtooth diagram of the past (Figure 4).

By tracking a single, stable, frequently hot pixel over the four-year span, we are able to map long-term changes in its dark current, in relation to each anneal period, as detailed in Figure 6. Here, once again, the vertical blue lines indicate the occurrence of an anneal while the black horizontal line indicates the hot-pixel threshold of 0.14 e^-/s. The inset diagram in the upper right portion of the plot serves as a visual representation of the WFC CCDs and reveals that this pixel, (x, y) = (1583, 3950), resides on WFC1. Immediately we notice this pixel's erratic behavior, fluctuating between several specific dark rate quantized states. Initially the pixel's dark current moves between being hot ($\approx$ 0.5 e^-/s) and super hot ($\geq$ 2.3 e^-/s) over the year-and-a-half period from January 2015 to July 2016. From July 2016 to March 2017, the pixel's dark current appears to stabilize around 1.9 e^-/s, and from March 2017 to January 2019 it hovers between 1.2 and 1.4 e^-/s.

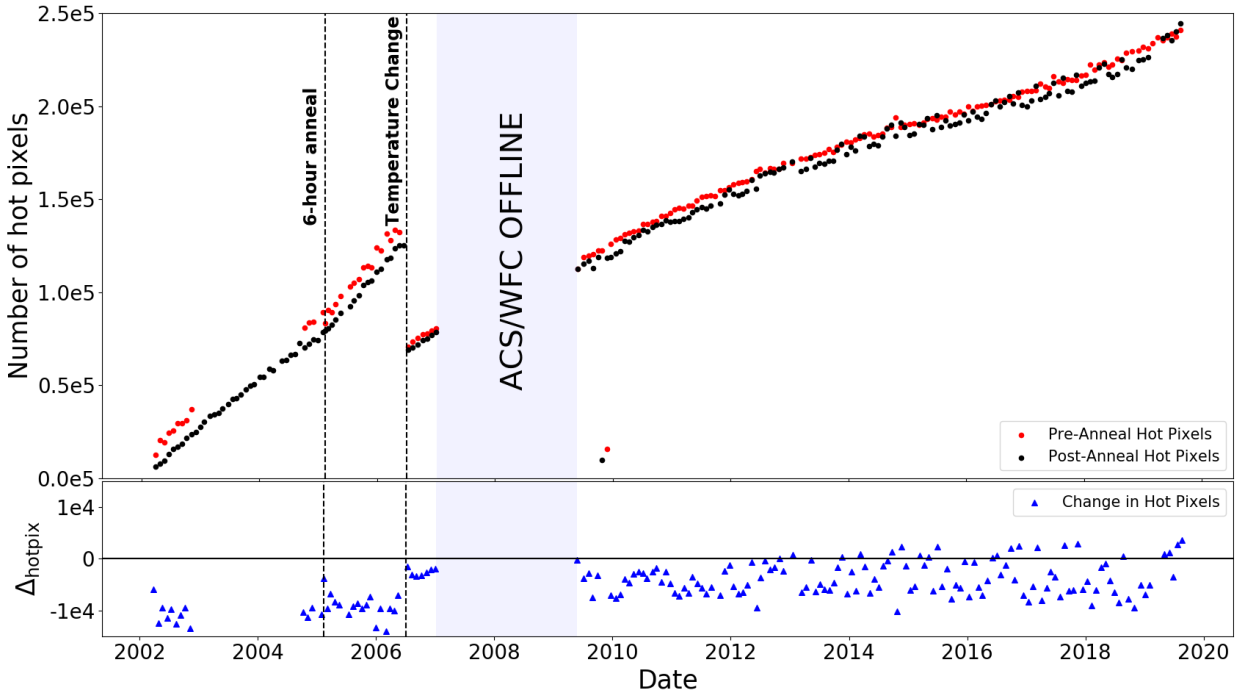

Figure 3: The total number of hot pixels pre- and post-anneal are plotted alongside the change in hot pixels (Δ_{hotpix}) for that anneal period. Each data point is a calibrated and combined stack of long dark frames from which the total hot pixel count is measured. Red points indicate pre-anneal hot pixels, black points indicate post-anneal hot pixels, and blue triangles (in the bottom panel) represent the change in hot pixels. All graph features including dashed lines and rectangles retain the same meaning as explained in Figure 1.

4 Discussion

In all of the pre- and post-anneal comparison plots, we observe the expected, linear increase in dark current from March 2002 to August 2019. In Figures 1 and 2, we see systematically higher dark rates in the mean measurements as compared to the median measurements; an expected result when pixels with very high dark currents are used in calculating the mean. The discrepancy between dark current measurements taken with respect to each readout amplifier as shown in Figure 2 and Table 2 may be attributed to the fact that each readout amplifier has unique readout electronics.

Seen most visibly in Figure 3, it is apparent that in the past several years, there have been many occasions when the post-anneal hot pixel count has been greater than its pre-anneal value. In fact, of the 85 anneals from January 2013 to August 2019 there have been 20 of these instances, despite zero occurring in the 12-year period prior. This means that 24% of anneals executed since 2013 have not been effective in reducing the dark current and hot pixel count in the ACS/WFC. This recent trend of increasing anneal ineffectiveness is problematic and, if left unmonitored, has the potential to contribute to calibration difficulties and noisier science images.

While we are not certain why recent anneals have not been as effective as they once were, we suspect that a contributing factor may be the inconsistencies that exist in the

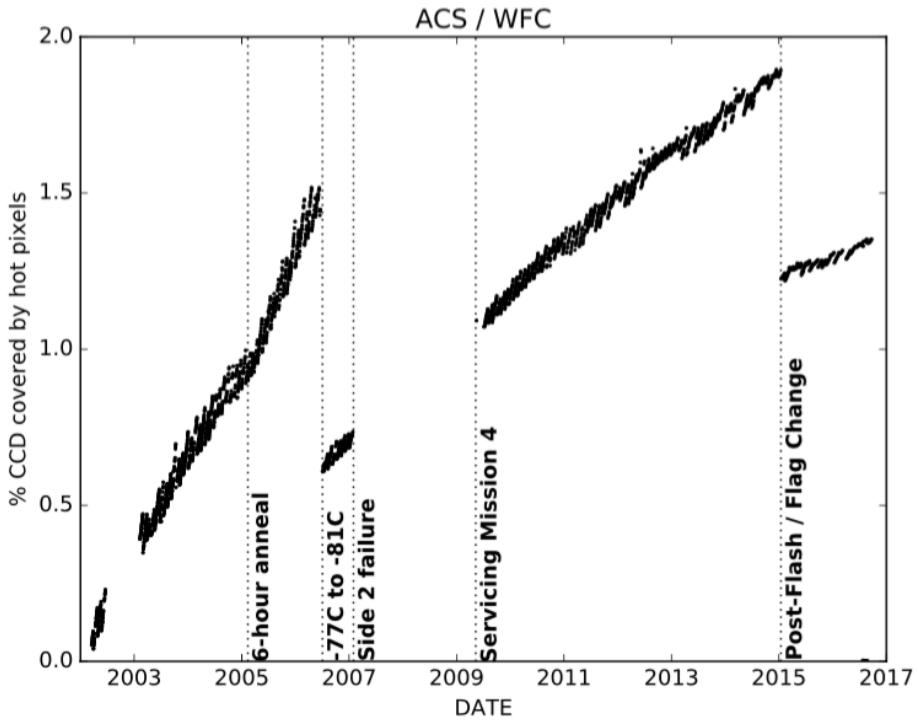

Figure 4: Percent hot pixel coverage in the ACS/WFC, also known as the sawtooth diagram, from 2002 to 2017 reproduced from the ACS Instrument Handbook (Ryon et al., 2018). The dotted vertical lines signify changes to ACS functionality over the instrument's lifetime that affected hot pixel growth. The data presents a sawtooth pattern because of the linear increase in hot pixels between anneal cycles, followed by the periodic reduction in hot pixels after each anneal occurs.

scheduling of the pre- and post-anneal dark frames. Beginning post-SM4 in late 2009, the anneal proposals request that four pre-anneal dark images must be taken within the 12-hour window before the anneal. The post-anneal frames, however, are scheduled to be taken anywhere from 6-18 hours after the anneal. This large window of time introduces possible inconsistencies in the data, particularly if some post-anneal darks are taken just six hours following an anneal and others are taken in double that time, or more.

When comparing the original ACS/WFC sawtooth diagram (Figure 4) to the reproduced one (Figure 5), although formatted differently and taking place over different date ranges, it is apparent that the original sawtooth diagram has a much tighter, cleaner zig-zag appearance than the sawtooth diagram produced from this analysis. The large amount of scatter seen between anneals in the reproduced sawtooth diagram is due, in part, to the fact that we are plotting percent hot pixel coverage from all 4 of the individual dark frames taken in a day, whereas the original sawtooth diagram plots the average of the 4 darks taken each day. Moreover, the method used to measure hot pixel count is different for both plots; the original sawtooth diagram categorizes hot pixels as those with a dark current that simply exceeds the hot pixel threshold, while our version uses a method that first weeds out cosmic rays using spatial parameters and then applies the hot pixel threshold. Despite these known differences between the two versions, some scatter in our plot remains and would require further investigation to determine a cause.

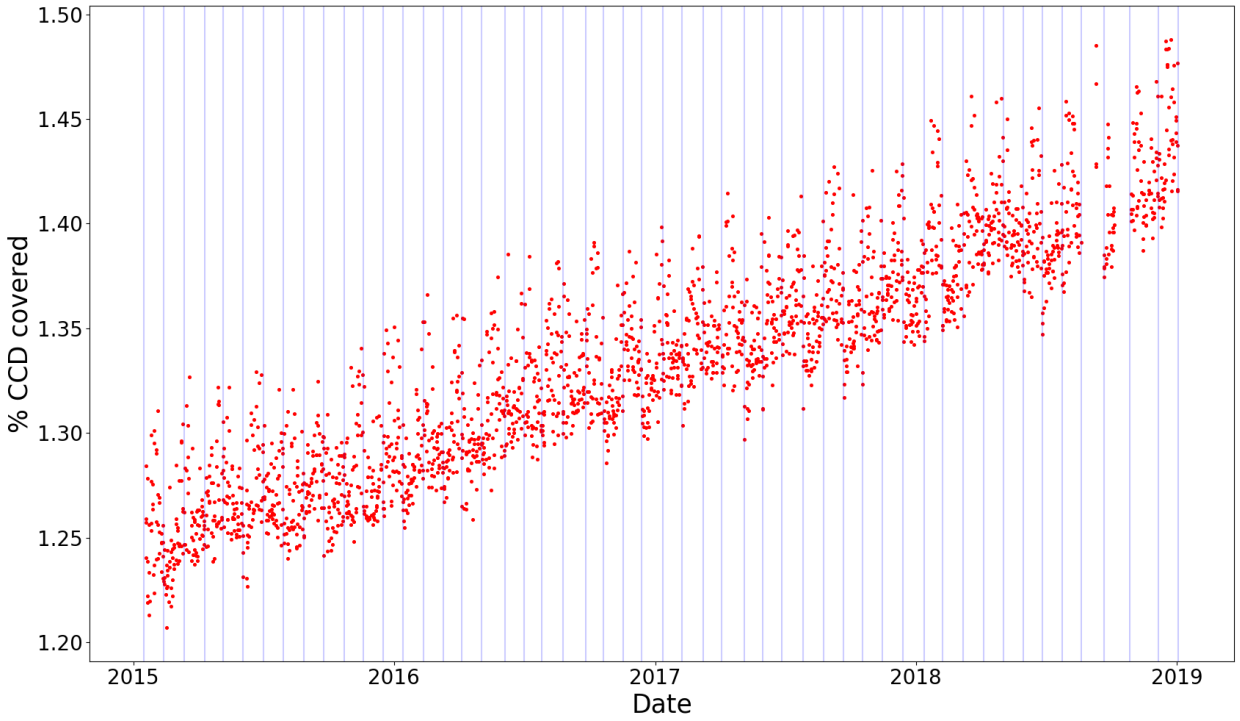

Figure 5: An updated version of the sawtooth diagram (Figure 4), this figure shows the percent of the WFC CCD detector area covered in hot pixels over a four-year period. Blue vertical lines indicate the occurrence of an anneal. Each red point uses the total hot pixel count from a single Daily Monitor dark frame to calculate percent hot pixel coverage.

By examining the changes in dark current that a single, stable, frequently hot pixel experiences over a four-year period, we see no predictable long-term pattern that emerges. As seen in Figure 6, the tracked pixel initially jumps back and forth between being hot and extremely hot, varying nearly 2.0 e^-/s each oscillation. It then stabilizes at a dark current value considered to be very hot before then stabilizing again at a reduced, but still very hot, dark current value. The erratic behavior that this pixel exhibits leads us to believe that pixels of the same classification, i.e., stable, hot and frequently hot, have highly unpredictable dark currents over long time scales. To fully understand the long-term behavior of hot pixels in the ACS/WFC, several examples of hot pixels with varying characteristics (i.e., combinations of unstable/stable, hot/very hot and frequently hot/infrequently hot) would need to be studied. Further analysis would allow for better pixel flagging in the calibration pipeline and a deeper understanding of how dark current in individual pixels changes over time in CCD detectors.

5 Conclusion

In this report, we use a collection of pre- and post-anneal dark frames, taken between the installation of ACS in 2002 and August 2019, to assess the efficacy of anneals in reducing the dark current and total number of hot pixels in the ACS/WFC. We confirm a steady, linear increase in dark current over the lifetime of ACS, peaking at 0.035 e^-/s in the mean and 0.014 e^-/s in the median. Generally speaking, the mean dark current of the detector is found to be

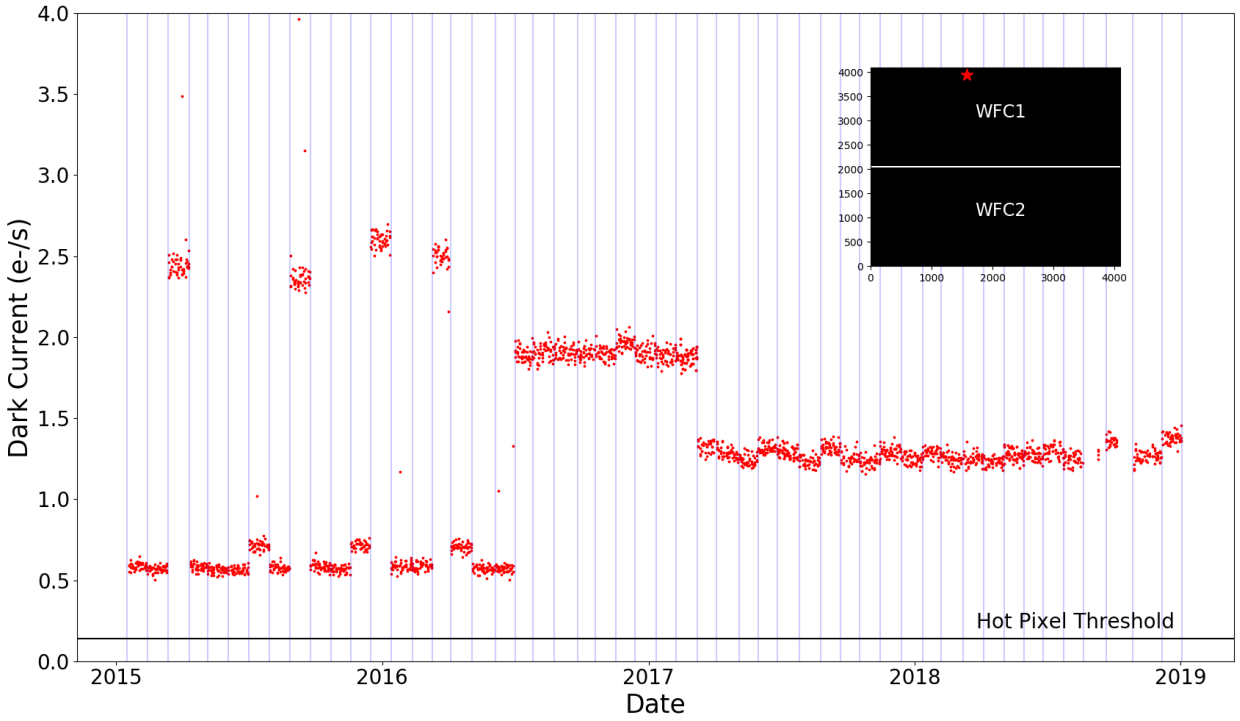

Figure 6: The dark current of a single, stable, frequently hot pixel is mapped over a four-year period. Like Figure 5, the blue vertical lines indicate the occurrence of an anneal. The black horizontal line denotes the hot pixel threshold of 0.14 e^-/s. The subplot in the right-hand corner of the figure illustrates that the tracked pixel exists on WFC1, with $(x, y) = (1583, 3950)$. This pixel exhibits large, unpredictable fluctuations in dark current over long time scales, transitioning from hot to extremely hot on several occasions.

consistently greater than the median, and the mean and median dark current is highest with respect to readout amplifier B, followed by amplifiers D, C and A. By comparing the total number of hot pixels pre- and post-anneal, we determine that 24% of anneals executed since 2013 show higher hot pixel counts after the anneal, than before. Based on these findings, we conclude that anneals in the last several years have proven less effective in reducing the dark current and number of hot pixels in the ACS/WFC as compared to the anneals carried out within the first 12 years of ACS functionality. We theorize that a large post-anneal scheduling window may contribute to inconsistent characterization of anneal efficacy in recent years, so further investigation into this is recommended.

We also investigate how using four years' worth of individual, Daily Monitor dark frames in conjunction with a unique hot pixel identifying method allows for the quantification, measurement and location of hot pixels in the WFC CCDs. Using the percent hot pixel coverage for each frame, we recreate the ACS/WFC sawtooth diagram where we observe the characteristic zig-zag pattern of the original, but with much more scatter present between anneals. We also identify a single, stable, frequently hot pixel and track its dark current from January 2015-2019. Due to the erratic behavior of this pixel's dark current, at times varying nearly 2.0 e^-/s over an anneal period, we determine that pixels of this classification likely have highly variable dark currents over time. A more well-rounded investigation into the behavior of hot pixels with varying levels of stability, frequency and signal is recommended

to provide better insight into the incidence and prevalence of hot pixels in the ACS/WFC.

6 Acknowledgements

The authors would like to thank Norman Grogin for his guidance and support throughout this project. Additionally, the authors would like to thank the following ACS team members for their helpful comments on this report: Nimish Hathi, Ralph Bohlin, Jenna Ryon, Melanie Olaes and Yotam Cohen.

References

Borncamp, D., Grogin, N., Bourque, M., & Ogaz, S. 2017, Pixel History for Advanced Camera for Surveys Wide Field Channel, Tech. Rep. ACS ISR 2017-05, STScI

Cox, C. 2002, CCD Hot Pixel Annealing, HST Proposal 9650

—. 2003, CCD Hot Pixel Annealing, HST Proposal 10046

Desjardins, T. D., Miles, N. D., Ryon, J. E., & Borncamp, D. C. 2018, ACS/WFC Superbias, Superdark, and Sink Pixel File Generation, Tech. Rep. ACS TIR 2018-01, STScI

Golimowski, D., Cheng, E., Loose, M., et al. 2011, ACS after Servicing Mission 4: The WFC Optimization Campaign, Tech. Rep. ACS ISR 2011-04, STScI

Ryon, J., et al. 2018, ACS Instrument Handbook, 17th edn. (STScI)

Sirianni, M., Gilliland, R., & Sembach, K. 2006, The ACS Side-2 Switch: An Opportunity to Adjust the WFC CCD Temperature Setpoint, Tech. Rep. ACS TIR 2006-02, STScI